ELSEVIER

Biophysical Chemistry 69 (1997) 107–124

Biophysical Chemistry

Nucleotide binding to IAF-labelled Na^+/K^+-ATPase measured by steady state fluorescence quenching by TNP–ADP

Edward H. Hellen, Promod R. Pratap *

Department of Physics and Astronomy, University of North Carolina at Greensboro, Greensboro, NC 27412, USA

Received 24 February 1997; revised 20 May 1997; accepted 20 May 1997

Abstract

Nucleotide binding to 5-iodoacetamidofluorescein (IAF) labelled Na^+/K^+-ATPase was measured by steady state fluorescence quenching of the fluorescein label via energy transfer to trinitrophenyl (TNP) labelled nucleotide. TNP-nucleotides are valuable probes of nucleotide binding to ATPases. Interpretation of these and other experiments in our laboratory using TNP-nucleotides with the Na^+/K^+-ATPase rely on having a good model for the interaction of TNP-nucleotide with the enzyme. Sets of fluorescence quenching curves obtained by titrating the enzyme with TNP–ADP in the presence of various concentrations of ADP could not be adequately modelled using a simple model with a single nucleotide binding site. Therefore, we compare various models which allow for additional TNP-nucleotide binding to the enzyme. In the two-site model, the additional binding is to a second specific site for which TNP-nucleotide and unlabelled nucleotide compete. In two other models, the additional binding (in one case saturable, and in the other case non-saturable) of TNP-nucleotide is not blocked by or affected by unlabelled nucleotide, and is, therefore, referred to as non-specific binding of the TNP-nucleotide. The goal of this work is to determine which of the distinctly different physical pictures associated with these models most accurately describes the interaction of TNP-nucleotide with the enzyme. We find that the interaction of TNP–ADP with IAF-labelled Na^+/K^+-ATPase is best described by a model in which there are two classes of binding: TNP–ADP and ADP compete for a specific binding site with dissociation binding constants of 0.13 μM for TNP–ADP and 2.0 μM for ADP; and non-saturable non-specific binding of TNP–ADP. © 1997 Elsevier Science B.V.

Keywords: Non-specific binding; Fluorescence energy transfer; Trinitrophenyl; Substrate binding

1. Introduction

The Na^+/K^+-ATPase is a primary active transport enzyme which uses energy from the hydrolysis of ATP to pump Na^+ and K^+ against their electrochemical gradients. During this process, the protein binds substrate (ATP) and releases product (ADP and inorganic phosphate) [1,2]. While the overall energetics of the reaction cycle of the enzyme can be accounted for by the energy of hydrolysis of ATP, partial reactions may be driven by energies of association and dissociation of various ligands. It is of interest, therefore, to measure the energies

* Corresponding author. Tel.: +1-910-334-5844; fax: +1-910-334-5865; e-mail: pratapp@dirac.uncg.edu

of binding and dissociation of these ligands. To this end, we are using fluorescence quenching of iodoacetamidofluorescein (IAF) labelled Na^+/K^+-ATPase via energy transfer to trinitrophenyl labelled ATP (TNP–ATP) and TNP–ADP to examine steady-state and transient ([3], submitted) kinetics of the enzyme nucleotide interaction. In this paper, we use the steady-state quenching data to determine the best model for the interaction of TNP-nucleotide with the enzyme. In addition to giving insight into the nature of this interaction, obtaining a good model is necessary for the analysis of the transient kinetic experiments.

When Na^+/K^+-ATPase labelled with iodoacetamidofluorescein (IAF) is mixed with TNP–ADP or TNP–ATP, IAF fluorescence is quenched via energy transfer to TNP-nucleotide bound to the enzyme [4]. In this paper, we titrate IAF-enzyme with TNP–ADP in competition with ADP. A simple model consisting of a single nucleotide binding site does not fit the fluorescence quenching data. Therefore, we compare three extensions of this simple model, each of which represents a distinctly different physical picture for the interaction of TNP-nucleotide with the enzyme. These physical pictures all contain the specific binding site from the single site model combined with either: a second specific nucleotide binding site for which nucleotide and TNP-nucleotide compete; or saturable non-specific binding of TNP-nucleotide; or non-saturable non-specific binding of TNP-nucleotide, where the non-specific binding is defined as the binding of TNP-nucleotide which is not blocked by or affected by unlabelled nucleotide.

An alternative method for measuring the interaction of TNP-nucleotide with enzyme is to measure the intrinsic fluorescence of the TNP-nucleotide. TNP-nucleotide has low fluorescence when free in aqueous buffer and undergoes a fluorescence enhancement when it binds to enzyme. Moczydlowski and Fortes [5,6] used this method to investigate nucleotide binding to the Na^+/K^+-ATPase. This method is complimentary to the quenching method we use here. There are two advantages of the quenching method. First, fluorescein is much more fluorescent than the TNP-nucleotides, so that the fluorescence signal is much larger from IAF-labelled enzyme than from TNP-nucleotide bound to the enzyme. Second, if TNP fluorescence is being monitored, then the TNP-nucleotide free in solution provides a background fluorescence which becomes a larger fraction of the total fluorescence as the concentration of TNP-nucleotide is increased beyond the amount needed to saturate the specific binding. Once the specific sites are saturated, further increases of the TNP-nucleotide concentration only obscure the signal from TNP-nucleotide bound to the enzyme. However, if IAF is being monitored, the increasing background signal from the TNP-nucleotide in solution is still small compared to the signal from the highly fluorescent IAF-labelled enzyme. Thus, higher concentrations of TNP-nucleotide can be investigated if fluorescence from IAF-labelled enzyme is monitored.

TNP-labelled nucleotides are useful probes for investigating nucleotide binding in a variety of ATPases. Other investigations using TNP-nucleotide to study the Na^+/K^+-ATPase include, Fortes and Aguilar [4] using quenching of IAF-labelled Na^+/K^+-ATPase by TNP–ATP to study nucleotide binding, and Amler et al. [7] using TNP–ATP in fluorescence energy transfer distance measurements. TNP-nucleotide investigations of other ATPases include the Ca^{2+}- ATPase [8], the F1-ATPase [9], and the H^+-ATPase [10]. So the characterization of the interaction of TNP-nucleotide with enzyme presented here may be of a more general interest.

Although our goal is to characterize the interaction of TNP-nucleotide with IAF-Na^+/K^+-ATPase for use in interpreting transient kinetic data, these results are relevant to issues concerning the number of nucleotide binding sites that exist on the enzyme. ATP plays two roles during the enzyme reaction cycle: (a) at high affinity ($K_d \approx 0.1 \pm 0.2$ μM), it binds to the enzyme in its Na^+-sensitive (traditionally, E_1) conformation and phosphorylates it; and (b) at low affinity ($K_d \approx 0.2 \pm 0.5$ mM) it binds to the K^+-sensitive (traditionally, E_2) conformation and it accelerates K^+ deocclusion from the enzyme. While the generally preferred explanation has been that ATP binds to a single site which changes its affinity during the reaction cycle [5], some recent evidence suggests that two sites coexist on the protein [11–13].

The results presented here for the fluorescence quenching of IAF-Na^+/K^+-ATPase via energy transfer to TNP-nucleotide show that there is substantial quenching which cannot be accounted for by just a single nucleotide binding site. It is necessary to include additional binding of TNP-nucleotide to the enzyme. This additional binding is best modelled as non-saturable and not blocked by or affected by unlabelled nucleotide.

We refer to this as non-specific binding of TNP-nucleotide to the enzyme, as opposed to the specific binding which can be blocked by unlabelled nucleotide. The specific nucleotide binding site is characterized by competition between TNP-nucleotide and unlabelled nucleotide for the site, with dissociation equilibrium constants of 0.13 μM for TNP–ADP and 2.0 μM for ADP. With this model, we can estimate the contributions of the high affinity specific and low affinity non-specific binding of TNP-nucleotide in stopped flow fluorescence quenching experiments ([3], submitted).

2. Models for fluorescence quenching

Here, we present the models used to analyze the fluorescence quenching data. First, we develop the simplest possible model of nucleotide binding, one with a single nucleotide binding site. While this model did not adequately fit the data, it provides the basis for the other models, and defines many of the parameters used in these models. These models are: a two-site model in which nucleotide and TNP-nucleotide compete for both sites; and two models which have a single specific site plus additional binding of TNP-nucleotide which is not blocked by or affected by unlabelled nucleotide. Since unlabelled nucleotide does not compete for this additional binding of TNP-nucleotide we refer to it as non-specific binding. Each of these extensions to the simple single site model uses a distinctly different physical picture of the interaction of TNP-nucleotide with the enzyme. Details of the derivations are in Appendix A.

In the models which include non-specific binding of TNP-nucleotide to the enzyme, we consider two extreme cases for the nature of the non-specific binding. Non-specific binding may be saturable due to a limited number of 'sites' at which the TNP-nucleotide can bind non-specifically. We model this case by allowing only one TNP-nucleotide to bind non-specifically to the enzyme. At the other extreme, non-specific binding may be non-saturable due to a virtually unlimited number of sites to which the TNP-nucleotide may non-specifically bind. This case is most simply modelled by making the concentration of non-specifically bound TNP-nucleotide linearly proportional to the bulk concentration [14,15]. A better approximation is to recognize that the surface of the enzyme is heterogeneous and therefore, the non-specific sites will likely have different affinities for TNP-nucleotide. This means the concentration of non-specifically bound TNP-nucleotide should not be linearly proportional to the bulk concentration, but instead must have a negative curvature. We include this feature in our non-saturable non-specific binding model. The saturable non-specific binding also has a negative curvature, however, it asymptotically approaches a maximal value, whereas the non-saturable non-specific binding has no asymptotic limit.

All of the models contain the following features: (1) Competition between acceptor labelled nucleotide (TNP-nucleotide) and unlabelled nucleotide for specific nucleotide binding site(s) on the donor-labelled enzyme; and (2) An 'inactive' fraction of enzyme whose specific binding site or sites cannot bind nucleotide. Many purification protocols inevitably cause some denaturation of enzyme, and it is important to take this into account [15]. In our case, the inactive fraction accounts for enzyme which had its nucleotide binding site denatured. The models which include non-specific binding also contain the following features: (1) Quenching due to non-specific binding of the TNP-nucleotide to the enzyme; and (2) Separate energy transfer parameters for specifically bound and non-specifically bound TNP-ADP. In all cases, the concentration of enzyme is small, so it is valid to assume that the concentrations of free and total ligand are the same.

2.1. Single site model

In this model, the IAF-labelled enzyme has a single specific nucleotide binding site for which TNP-nucleotide (the fluorescence quencher) and unlabelled nucleotide compete. There is no non-specific binding of

TNP-nucleotide. The specific binding is saturable and is characterized by the standard equilibrium dissociation constant K

$$E + \mathrm{L} \rightleftharpoons E\mathrm{L} \tag{1}$$

with

$$K = \frac{[E][\mathrm{L}]}{[E\mathrm{L}]} \tag{2}$$

where the ligand L represents either unlabelled nucleotide or TNP-nucleotide. Appendix A shows that when IAF-enzyme is in the presence of the TNP-nucleotide and unlabelled nucleotide, the normalized fluorescence for the single site model is

$$f(A,T,Ka,Kt,k_1,xa) = (1 - xa) + xa\left(\frac{1 + \dfrac{A}{Ka} + \dfrac{T}{Kt}\dfrac{1}{1+k_1}}{1 + \dfrac{A}{Ka} + \dfrac{T}{Kt}}\right) \tag{3}$$

where A and Ka are the concentration and equilibrium dissociation constant for unlabelled nucleotide, T and Kt are the corresponding parameters for TNP-labelled nucleotide, k_1 is the deexcitation rate constant due to energy transfer from the IAF-labelled enzyme to the TNP-nucleotide (normalized with respect to the inverse of the unquenched fluorescence lifetime of the IAF-labelled enzyme), and xa is the fraction of IAF-enzyme which can bind nucleotide. The first term in Eq. (3) represents the fluorescence from inactive enzyme, and the second term represents fluorescence from active enzyme.

2.2. Two-site model

In this model, the enzyme has two nucleotide binding sites, 1 and 2, each with its own equilibrium constants, Ka_1 and Ka_2 for nucleotide, and Kt_1 and Kt_2 TNP-nucleotide, and its own normalized energy transfer deexcitation rate constants, k_1 and k_2. For the inactive fraction of enzyme, neither site can bind nucleotide. There is no non-specific binding of TNP-nucleotide. The normalized fluorescence for the two-site model is

$$\begin{aligned} f(A,T,Ka_1,Kt_1,Ka_2,Kt_2,k_1,k_2,xa) = {} & (1 - xa) \\ & + xa\left(\frac{1 + \dfrac{A}{Ka_1} + \dfrac{A}{Ka_2} + \dfrac{A^2}{Ka_1 Ka_2} + \left(\dfrac{T}{Kt_1} + \dfrac{T}{Kt_1}\dfrac{A}{Ka_2}\right)\dfrac{1}{1+k_1}}{1 + \dfrac{A}{Ka_1} + \dfrac{A}{Ka_2} + \dfrac{A^2}{Ka_1 Ka_2} + \dfrac{T}{Kt_1} + \dfrac{T}{Kt_1}\dfrac{A}{Ka_2} + \dfrac{T}{Kt_2} + \dfrac{A}{Ka_1}\dfrac{T}{Kt_2} + \dfrac{T^2}{Kt_1 Kt_2}}\right) \\ & + xa\left(\frac{\left(\dfrac{T}{Kt_2} + \dfrac{A}{Ka_1}\dfrac{T}{Kt_2}\right)\dfrac{1}{1+k_2} + \dfrac{T^2}{Kt_1 Kt_2}\dfrac{1}{1+k_1+k_2}}{1 + \dfrac{A}{Ka_1} + \dfrac{A}{Ka_2} + \dfrac{A^2}{Ka_1 Ka_2} + \dfrac{T}{Kt_1} + \dfrac{T}{Kt_1}\dfrac{A}{Ka_2} + \dfrac{T}{Kt_2} + \dfrac{A}{Ka_1}\dfrac{T}{Kt_2} + \dfrac{T^2}{Kt_1 Kt_2}}\right) \end{aligned} \tag{4}$$

where A, T, and xa are as defined in the single site model.

2.3. Single site plus saturable non-specific binding model

In addition to the single specific nucleotide binding site on the active IAF-enzyme, in this model only one TNP-nucleotide can bind non-specifically to each IAF-enzyme, both active and inactive. This describes

saturable non-specific binding of TNP-nucleotide which is characterized by an equilibrium dissociation constant Kt_2 and a normalized energy transfer deexcitation rate constant k_2. Unlabelled nucleotide does not block or affect the non-specific binding of TNP–ADP to the enzyme. The normalized fluorescence for the single site plus saturable non-specific binding model is

$$f(A,T,Ka_1,Kt_1,Kt_2,k_1k_2,xa) = (1-xa)\left(\frac{1+\frac{T}{Kt_2}\frac{1}{1+k_2}}{1+\frac{T}{Kt_2}}\right) + xa\left(\frac{1+\frac{A}{Ka_1}+\frac{T}{Kt_1}\frac{1}{1+k_1}+\left(\frac{T}{Kt_2}+\frac{A}{Ka_1}\frac{T}{Kt_2}\right)\frac{1}{1+k_2}+\frac{T^2}{Kt_1Kt_2}\frac{1}{1+k_1+k_2}}{1+\frac{A}{Ka_1}+\frac{T}{Kt_1}+\frac{T}{Kt_2}+\frac{A}{Ka_1}\frac{T}{Kt_2}+\frac{T^2}{Kt_1Kt_2}}\right) \quad (5)$$

where A, T, and xa are as defined above.

2.4. Single site plus non-saturable non-specific binding

In addition to the single specific nucleotide binding site on the active IAF-enzyme, in this model the number of TNP-nucleotide bound non-specifically to the IAF-enzyme, both active and inactive, increases without limit as the concentration of TNP-nucleotide in solution increases. This describes non-saturable non-specific binding of TNP-nucleotide which is characterized by two parameters, q and a, which are discussed in Appendix A. The normalized fluorescence for the single site plus non-saturable non-specific binding model is

$$f(A,T,Ka,Kt,k_1,q,a,xa) = \frac{(1-xa)}{1+qT^a} + xa\left(\frac{\left(1+\frac{A}{Ka}\right)\frac{1}{1+qT^a}+\frac{T}{Kt}\frac{1}{1+k_1+qT^a}}{1+\frac{A}{Ka}+\frac{T}{Kt}}\right) \quad (6)$$

where q and a are parameters which characterize the quenching due to non-specific binding, and the other parameters are as in the single site model.

3. Materials and methods

TNP–ADP and IAF were from Molecular Probes (Eugene, OR). Other chemicals were from Sigma (St. Louis, MO). Frozen dog kidneys were from Pel-Freez (Rogers, AR). Fresh dog kidneys were obtained locally.

IAF-labelled Na^+/K^+-ATPase was obtained as described earlier [16–18]. Enzyme concentrations used for fluorescence measurements were about 10 nM. The buffer contained 25 mM imidazole, pH 7.0, 140 mM choline chloride, 20 mM NaCl, and 1 mM EDTA. Activities were measured using a coupled fluorometric assay [19]. The activity for the preparations from Pel-Freez kidneys was 3–4 μM Pi/min/(mg enz), and from the fresh kidneys was 6–7 μM Pi/min/(mg enz) at 25°C.

3.1. Fluorescence measurements

Fluorescence intensities were measured on a QM-1 fluorescence spectrophotometer (PTI, Brunswick, NJ), with excitation at 490 nm and emission at 520 nm. Temperature was kept at 25°C with a circulating waterbath.

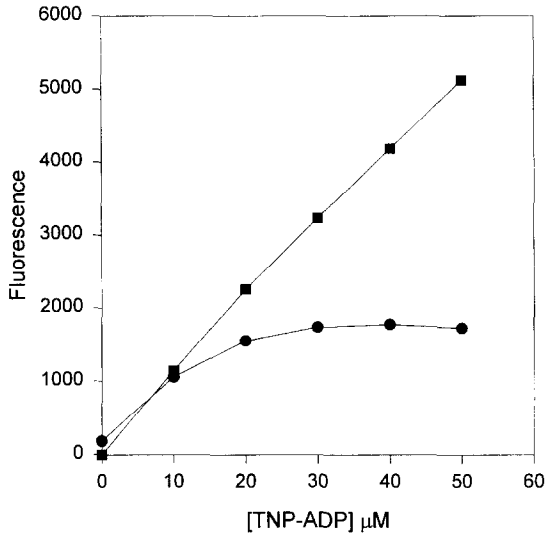

Fig. 1. TNP–ADP fluorescence, uncorrected (●) and corrected (■), vs. TNP–ADP concentration. Linearity of the corrected fluorescence demonstrates that the inner filter corrections described in Section 3 are appropriate.

A stirring bar was run continuously in the cuvette.

Due to the high concentrations of TNP-nucleotide used in the titrations (up to 50 μM) and the overlap of its spectral properties with those of fluorescein, care must be used in the corrections to the raw fluorescence data. Corrections are made for: contribution of TNP fluorescence, dilution caused by the titrations, energy transfer from IAF to TNP free in solution, and the inner filter effect for both excitation and emission. Control experiments provide parameters needed in these corrections. All these corrections will be described, then combined into a single equation.

The absorption at 490 nm and 520 nm was linear with TNP concentration over the range of the titration, and provided the extinction coefficients needed for the inner filter corrections for excitation and emission in fluorescence measurements. TNP–ADP was titrated into buffer containing no fluorescein while fluorescence was measured with excitation at 490 nm and emission at 520 nm. Fig. 1 shows that after correction for dilution and inner filter effects, the TNP fluorescence was linear with TNP concentration, as expected. This demonstrated that these corrections were accurate and also provided information necessary for the corrections due to TNP fluorescence in experiments with IAF-labelled enzyme.

Fluorescence decrease due to energy transfer from IAF to TNP free in solution was checked by titrating TNP–ADP into buffer containing IAF while fluorescence was measured with excitation at 490 nm and emission at 520 nm. Fig. 2 shows that after corrections for inner filter effects, dilution, and TNP fluorescence, the fluorescence showed a decline instead of being constant as one would expect if there was no energy transfer from IAF to TNP. The following estimation shows that this decrease in fluorescence is expected due to energy transfer from the highly fluorescent IAF to the low fluorescence TNP. The fraction of excited IAF molecules which are quenched can be found by dividing the effective quenching volume of a TNP by the total volume per TNP. At 50 μM TNP, the total volume per TNP is 30,000 nm^3. The effective quenching volume is a sphere whose radius is a combination of the characteristic energy transfer distance and the root-mean-square distance for diffusion during the fluorescence lifetime, $\langle x \rangle = (4D\tau)^{1/2}$. Using a characteristic transfer distance of 6 nm, a diffusion coefficient of 1×10^{-5} cm^2/s, and a fluorescence lifetime of 4 ns gives a quenching volume of 4000 nm^3. Thus at 50 μM TNP, 13% of the excited IAF will be quenched. This estimate agrees well with the 15% shown in Fig. 2 at 50 μM TNP. The normalized IAF fluorescence as a function of TNP concentration over

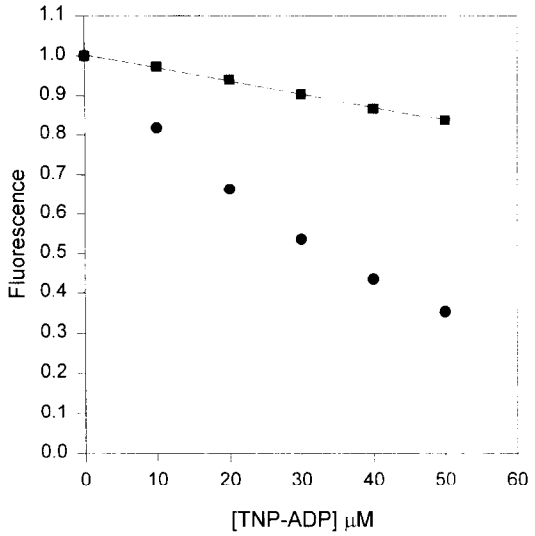

Fig. 2. Fluorescence from free IAF, uncorrected (●) and corrected (■), vs. TNP–ADP concentration. Also shown is the best fit straight line parameterization used to correct for energy transfer from IAF to TNP–ADP free in solution, as described in Section 3.

the range of the titration was found to be well paramaterized by $f([\mathrm{TNP}]) = 1 - 0.0031[\mathrm{TNP}]$ where [TNP] is in units of μM.

For IAF bound to enzyme, an estimate of the quenching due to TNP free in solution is made by adjusting the quenching volume to take into account the decreased access that TNP has to IAF due to the adjacent volume occupied by the membrane and cytoplasmic portion of the enzyme. IAF is bound to the cytoplasmic portion of the enzyme close to the membrane [4]. The membrane alone reduces the quenching volume accessible to TNP by a factor of two. The cytoplasmic portion of the enzyme occupies approximately half of the remaining quenching volume thus contributing another factor of two. So the expected normalized fluorescence decrease due to energy transfer from IAF-labelled enzyme to TNP free in solution is $f([\mathrm{TNP}]) = (1 - 0.0031/4)[\mathrm{TNP}]$. Correction for this energy transfer is accomplished by dividing the data by this parameterization.

The complete correction to the raw data is obtained by combining the above corrections, which results in the corrected fluorescence

$$F = \frac{1}{1 - \frac{0.0031}{4}[\mathrm{TNP}]}\left(\frac{V(\mathrm{TNP})}{V_0}(\mathrm{raw} - \mathrm{dark})10^{(\varepsilon_{490}+\varepsilon_{520})\frac{1}{2}[\mathrm{TNP}]} - f_{\mathrm{tnp}}([\mathrm{TNP}])\right) \tag{7}$$

where $V(\mathrm{TNP})$ is the sample volume as a function of the TNP concentration, V_0 is the initial volume with no TNP, ε_{490} and ε_{520} are extinction coefficients determined in the control experiments, *dark* is the background signal with the excitation blocked, and f_{TNP} is the TNP fluorescence determined in the control experiments. The $1/2$ in the inner filter correction term is because the path length for excitation and emission are each 0.5 cm.

Curve fitting was done by simultaneously minimizing the sum of the square of the errors for complete sets of fluorescence quenching data curves including all the concentrations of ADP. Minimization routines using the Levenberg algorithm were used from both Sigmaplot (Jandel Scientific) and Mathcad (MathSoft). The standard errors for the best fit parameters, the parameter dependencies, and the reduced χ^2 values for the best fits were found and used to evaluate the quality of the fits. Uncertainties were 0.3% for the uncorrected normalized fluorescence and were increased in accordance with the above corrections to the fluorescence.

The parameters xa for the active fraction and k_1 for the energy transfer rate were found to be dependent such that when both were free parameters in the curve fitting, one could be increased and the other decreased such that the other parameters did not change significantly and the quality of the fit was unaffected. (For example, in one trial xa could be increased from 0.40 to 1.0 while k_1 was decreased from 20 to 0.66.) This dependency was also indicated by their parameter dependencies being greater than 0.999. This just reflects the fact that in steady state fluorescence quenching, one cannot distinguish between a small fraction of heavily quenched fluorophore and a large fraction of less strongly quenched fluorophore. Therefore, it was necessary to apply some constraint on these dependent parameters. The measured enzyme activities provide some information about the active fractions, however, it is difficult to know what level of activity actually corresponds to an active fraction of 100%. Fluorescence lifetime measurements provide information about the energy transfer rate. Fortes and Aguilar [4] reported that the time resolved fluorescence decay for IAF-labelled Na^+/K^+-ATPase can be described by a single exponential with a lifetime of 4 ns and that in the presence of TNP-nucleotide, the fluorescence decay is described by two exponentials, 75% with the unquenched lifetime of 4 ns, and 25% with a lifetime of 1 ns. If $k_t = k_f + k_q$ is the total decay rate in the presence of the TNP quencher where k_f is the decay rate in the absence of quencher and k_q is the energy transfer rate then since $k_f = 1/(4\ \text{ns})$ and $k_t = 1/(1\ \text{ns})$, we have the normalized energy transfer decay rate $k_q/k_f = 3$. This was used as a constraint in the curve fitting, and the resulting active fractions were then checked to make sure they were consistent with the measured activities.

4. Results

Fig. 3 shows the fluorescence quenching data for IAF-labelled Na^+/K^+-ATPase as a function of TNP–ADP concentration in the presence of 0, 10, 50, and 4000 μM ADP. As the concentration of TNP–ADP increases from zero to 10 μM, the fluorescence decreases due to increased energy transfer from IAF to TNP. The presence of increasing amounts of ADP causes decreased TNP–ADP quenching of IAF fluorescence. Also

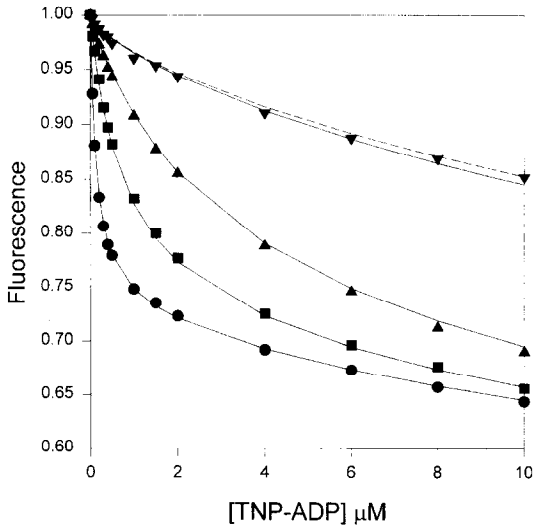

Fig. 3. Normalized fluorescence quenching data for IAF labelled Na^+/K^+-ATPase being titrated by TNP–ADP in the presence of 0 (●), 10 (■), 50 (▲), and 4000 (▼) μM ADP, and best fit using the single site plus non-saturable non-specific binding model. The dashed line is the quenching due to non-specifically bound TNP–ADP predicted by this model using the best fit parameters in Table 1.

Table 1
Curve fitting parameters. Best fit parameters, standard errors, and reduced chi square (χ_r^2) for the single site plus non-saturable non-specific binding model, the single site plus saturable non-specific binding model and the two-site model

Single site + non-saturable non-specific	Kt (μM)	Ka (μM)	q	a		xa	χ_r^2
Trial 1	0.136 ± 0.007	2.0 ± 0.1	0.028 ± 0.002	0.66 ± 0.02		0.219 ± 0.003	1.06
Trial 2	0.162 ± 0.006	2.3 ± 0.1	0.026 ± 0.001	0.65 ± 0.02		0.212 ± 0.002	0.53
Trial 3	0.130 ± 0.004	1.97 ± 0.06	0.037 ± 0.001	0.67 ± 0.01		0.342 ± 0.002	0.64
Trial 4	0.134 ± 0.005	3.1 ± 0.2	0.039 ± 0.001	0.69 ± 0.01		0.222 ± 0.002	0.62
Trial 5	0.093 ± 0.002	1.36 ± 0.04	0.023 ± 0.001	0.60 ± 0.02		0.548 ± 0.003	1.39
Trial 6	0.115 ± 0.002	1.50 ± 0.04	0.033 ± 0.001	0.56 ± 0.01		0.517 ± 0.002	0.90
Single site + saturable non-specific	Kt_1 (μM)	Ka_1 (μM)	Kt_2 (μM)		k_2	xa	χ_r^2
Trial 1	0.12 ± 0.01	2.0 ± 0.2	7 ± 1		0.22 ± 0.02	0.220 ± 0.004	1.59
Trial 2	0.15 ± 0.01	2.3 ± 0.2	7 ± 1		0.19 ± 0.01	0.210 ± 0.003	1.06
Trial 3	0.12 ± 0.01	1.9 ± 0.1	6 ± 1		0.29 ± 0.02	0.339 ± 0.003	1.69
Trial 4	0.13 ± 0.01	4.3 ± 0.5	23 ± 2		1.0 ± 0.1	0.235 ± 0.006	4.54
Trial 5	0.089 ± 0.003	1.39 ± 0.06	14 ± 2		0.27 ± 0.02	0.549 ± 0.004	2.82
Trial 6	0.107 ± 0.005	1.5 ± 0.1	10 ± 1		0.30 ± 0.02	0.518 ± 0.005	4.84
Two-site	Kt_1 (μM)	Ka_1 (μM)	Kt_2 (μM)	Ka_2 (μM)	k_2	xa	χ_r^2
Trial 1	0.22 ± 0.02	2.9 ± 0.3	11 ± 1	uncertain	uncertain	0.273 ± 0.004	4.7
Trial 2	0.25 ± 0.02	3.3 ± 0.4	12 ± 1	uncertain	uncertain	0.263 ± 0.004	4.04
Trial 3	0.18 ± 0.01	2.7 ± 0.2	14 ± 1	uncertain	uncertain	0.40 ± 0.01	6.2
Trial 4	0.48 ± 0.07	7 ± 2	12 ± 2	uncertain	uncertain	0.37 ± 0.01	35
Trial 5	0.099 ± 0.004	1.60 ± 0.07	58 ± 6	uncertain	uncertain	0.569 ± 0.005	4.45
Trial 6	0.125 ± 0.006	1.9 ± 0.1	36 ± 4	uncertain	uncertain	0.550 ± 0.006	5.81

shown is the best fit using the single site plus non-saturable non-specific binding model, Eq. (6). Best fit parameters, standard errors of the parameters, and reduced χ^2 values for the two-site model, the single site plus saturable non-specific binding model, and the single site plus non-saturable non-specific binding model for this experiment are shown in Table 1. Trial 3 is from the data in Fig. 3. (Parameters for the single site model are not shown since it was not able to fit the data.)

The dashed line in Fig. 3 shows the quenching due to non-specific binding of TNP–ADP predicted by the single site plus non-saturable non-specific binding model using the best fit parameters. This curve closely follows the data and fit for the case where specific binding is blocked by the presence of 4000 μM ADP.

Fig. 4 shows the fluorescence recovery when TNP–ADP is chased off of the enzyme by the addition of ADP. The ADP is added to the 'no ADP' sample from Fig. 3 at the end of the TNP–ADP titration. Also shown is the predicted fluorescence recovery using the best fit parameters from Table 1 for the single site plus non-saturable non-specific binding model. Note that the fluorescence recovers to nearly the same level as the final fluorescence in Fig. 3 for the TNP–ADP titration in the presence of 4000 μM ADP.

TNP–ADP titrations were done from zero to 50 μM in an attempt to clearly determine which of the non-specific binding models is the most accurate representation of the interaction of TNP–ADP with the enzyme. Fig. 5 shows fluorescence quenching data for a titration to 50 μM TNP–ADP in the presence of 0, 30, 100, and 1000 μM ADP. Note that the x-axis is plotted on logarithmic scale since the TNP concentration spans three decades. Also shown is the best fit using the single site plus non-saturable non-specific binding model. The best fit parameters, their standard errors, and the reduced χ^2 values for the various models are shown in Table 1 under Trial 6. The dashed line in Fig. 5 shows the quenching due to non-specific binding of TNP– ADP predicted by the single site plus non-saturable non-specific binding model using the best fit parameters.

Table 1 shows curve fitting results from experiments using different enzyme preparations and in the presence of different concentrations of ADP. Trials 1 and 2 are titrations to 10 μM TNP–ADP in the presence of 0, 5, 20

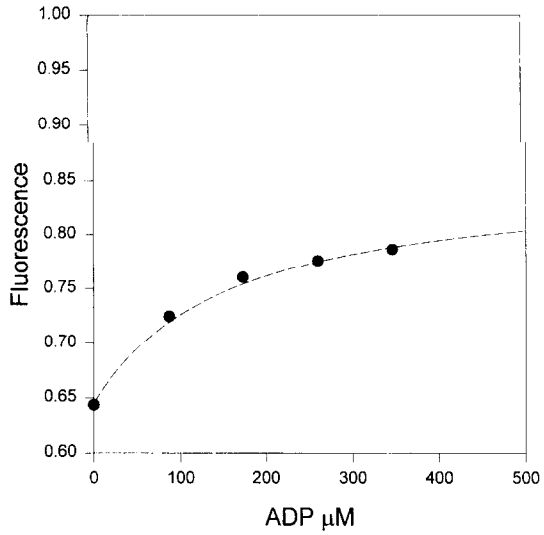

Fig. 4. Fluorescence recovery as ADP is added to the 'no ADP' enzyme sample from Fig. 3 at the end of the TNP–ADP titration. Also shown is the predicted recovery using the best fit parameters from Table 1 for the single site plus non-saturable non-specific binding model.

and 200 μM ADP. Trial 3 is discussed above. Trials 4, 5, and 6 are titrations to 50 μM TNP–ADP in the presence of 0, 30, 100 and 1000 μM ADP. Best fit parameters for Ka_2 and k_2 in the two-site model were undetermined due to complete uncertainty in their values based on their standard errors. The other parameters for this model and the quality of the fit did not significantly change when Ka_2 and k_2 were set to be infinite. Trials 1 through 4 used enzyme prepared from frozen dog kidneys. Trials 5 and 6 used enzyme prepared from fresh dog kidneys.

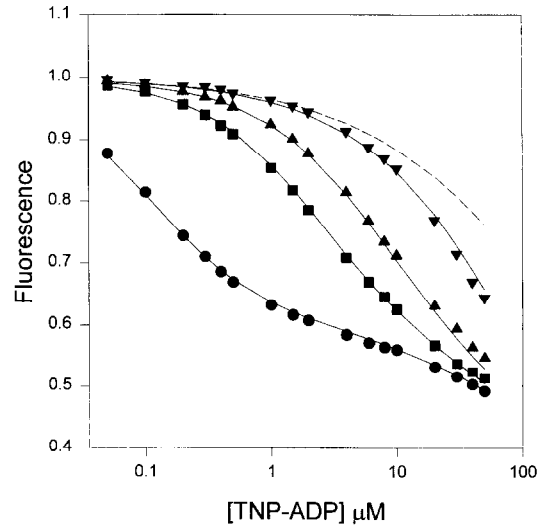

Fig. 5. Normalized fluorescence quenching data for IAF labelled Na^+/K^+-ATPase being titrated by TNP–ADP in the presence of 0 (●), 30 (■), 100 (▲), and 1000 (▼) μM ADP, and best fit using the single site plus non-saturable non-specific binding model. The dashed line is the quenching due to non-specifically bound TNP–ADP predicted by this model using the best fit parameters in Table 1.

5. Discussion

TNP labelled nucleotides are useful spectroscopic probes for investigating substrate binding in a variety of ATPases. We are using TNP-nucleotides in steady state and transient kinetics studies of the Na^+/K^+-ATPase. In this paper, we determine the best model for the interaction of TNP-nucleotide with Na^+/K^+-ATPase by fitting different models to data from the fluorescence quenching of IAF-labelled Na^+/K^+-ATPase via energy transfer to TNP–ADP in the presence of various concentrations of ADP. Each of the models represents a distinctly different physical picture of the interaction of TNP-nucleotide with the enzyme. Selection of the best model provides insight into the nature of this interaction, and is necessary for analysis of stopped flow fluorescence experiments which use TNP-nucleotide to measure transient kinetics of nucleotide binding to the Na^+/K^+-ATPase ([3], submitted).

A model in which TNP-nucleotide and unlabelled nucleotide compete for a single nucleotide binding site on the enzyme was not able to fit the data. Since during the Na^+/K^+ – ATPase's reaction cycle low-affinity and high-affinity nucleotide binding sites are demonstrable (at least sequentially), a natural extension of the single-site model is a two-site model in which TNP-nucleotide and unlabelled nucleotide compete for both sites. A distinctly different extension is suggested by the observation that when TNP–ADP is added to IAF-labelled enzyme in the presence of ADP, there is a substantial fraction of the quenching which cannot be stopped by increasing the concentration of ADP. In order to account for this, we use models that include additional binding of TNP–ADP, which is not blocked by or affected by ADP. We refer to this type of binding as non-specific. Reports of non-specific or non-saturable binding of TNP-nucleotide to the Na^+/K^+-ATPase [5], the cytoplasmic loop of Ca^{2+}-ATPase [8], and the ATP binding domain of H^+-ATPase [10] suggest that its explicit inclusion in a binding model is of general use.

Given that a model with only a single specific binding site is insufficient, so that additional binding of TNP-nucleotide to the enzyme is required, it is desirable to consider a broad range of possibilities for the nature of the additional binding. We attempt to do this by considering three possibilities for the additional binding: a second specific binding site; and two types of non-specific binding, saturable and non-saturable. The goal is to determine which of these distinctly different physical pictures most accurately describes the additional binding. We find that a model with a single specific nucleotide binding site plus non-saturable non-specific binding of TNP-nucleotide fit the data best.

5.1. Comparison of models

Table 1 shows that the models with non-specific binding fit the data better than the two-site model. The reduced χ^2 values for the single site plus non-saturable non-specific binding model are close to one in all trials, and for the single site plus saturable non-specific binding they are close to one when the titration was up to 10 μM TNP–ADP, but not when it was up to 50 μM TNP–ADP. For the two-site model, the reduced χ^2 value was unacceptable in all trials. In addition, the models with non-specific binding give better fits using one less parameter than the two-site model. These comparisons lead us to prefer the single site plus non-saturable non-specific binding model.

The values of the active fraction, xa, correlate well with the measured activities. The active fraction for the enzyme from freshly obtained dog kidney was 0.51 and 0.55, approximately two times that from enzyme prepared from purchased frozen dog kidneys, 0.23 and 0.34. This agrees well with the measured activities given in Section 3. These values also agree with active fractions based on ouabain binding experiments which require phosphorylation of the enzyme (in preparation).

An even simpler model which incorporates non-saturable non-specific binding is possible by setting $a = 1$ in Eq. (6) [14,15]. However, when we tried this with $a = 1$, the reduced χ^2 increased by almost factor of 10, from 1.1 to 9 for the titrations out to 50 μM TNP–ADP.

The usual method for finding the affinity constants in a competitive binding assay is to find apparent affinity constants by fitting each titration curve individually using a model with a single saturable site and no competing

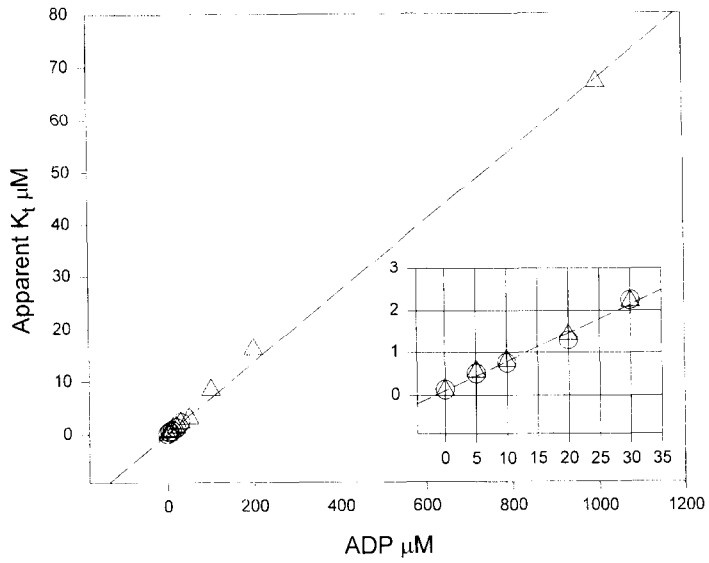

Fig. 6. Apparent affinity constant for TNP–ADP binding to IAF labelled Na^+/K^+-ATPase as a function of ADP concentration. Inset: Values determined by the usual method as described in text (○), and then fit to a straight line in order to determine the dissociation constants of 1.6 μM and 0.11 μM for ADP and TNP–ADP respectively from Eq. (9). Main: Apparent K_t for the higher concentrations of ADP could only be found when parameters for the non-specific binding were held fixed to values in Table 1 (△). Note how closely these apparent K_t values lie to the straight line fit from the inset.

ligand present [8,10]. At saturation some asymptotic behavior is approached, not necessarily constant or even linear. In our case, this method is accomplished by rewriting Eq. (6) as

$$f = \frac{1 - xa}{1 + qT^a} + \left(\frac{K_{t\mathrm{app}}}{K_{t\mathrm{app}} + T}\right)\frac{1}{1 + qT^a} + \left(\frac{T}{K_{t\mathrm{app}} + T}\right)\frac{1}{1 + k_1 + qT^a} \tag{8}$$

where

$$K_{t\mathrm{app}} = \frac{K_t}{K_a}[\mathrm{ADP}] + K_t \tag{9}$$

Fitting Eq. (8) to single titration curves for each concentration of ADP results in an apparent affinity constant, $K_{t\mathrm{app}}$, for the TNP–ADP which depends on the concentration of the ADP. Values for the true affinity constants K_t and K_a are obtained by fitting Eq. (9) to the values of $K_{t\mathrm{app}}$, versus [ADP]. At saturation of the specific binding site, the asymptotic behavior of the titration curve is accounted for by the non-specific binding parameters, q and a.

Fig. 6 shows the results from this alternate method. Values of $K_{t\mathrm{app}}$ were found by fitting individual titration curves to Eq. (8) for the various concentrations of ADP. $K_{t\mathrm{app}}$ values for ADP concentrations up to 30 μM (about 10 times the resultant dissociation constant, K_a, for ADP) were fit to Eq. (9) in order to determine K_t and K_a. The resultant values of 0.11 μM for K_t and 1.6 μM for K_a agree well with the values shown in Table 1 obtained by the global fitting method. However, for concentrations of ADP greater than 50 μM, it was not possible to find unique best fit solutions due to there being too many parameters in the model, Eq. (8), for these titration curves which, due to the blocking of most of the specific binding, are relatively featureless compared to the curves with low ADP. When the parameters characterizing the additional binding (i.e., q and a) were held fixed to the values shown in Table 1, thereby reducing the number of parameters, then values for $K_{t\mathrm{app}}$ were found for the titration curves with high ADP. These values are also shown in Fig. 6. Note how closely they lie

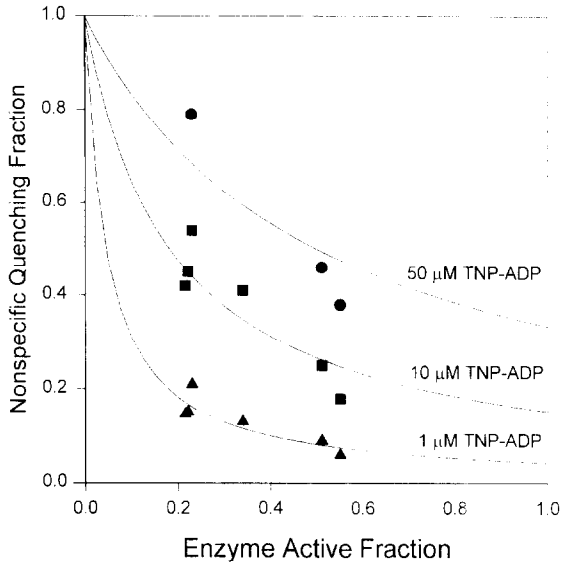

Fig. 7. Fraction of quenching due to non-specific binding of TNP–ADP to the IAF labelled Na^+/K^+-ATPase versus the active fraction of enzyme. Curves are calculated from the model in Eq. (6) as described in the text. Also shown are values measured from the TNP–ADP titration data for 1 μM (▲), 10 μM (■), and 50 μM (●) TNP–ADP.

to the straight line prediction from the fit of Eq. (9). So, it is clear that our global method gives the same results for the high affinity specific binding as the traditional method. However, we find our method more convenient for comparing the various models here because we avoid having to impose constraints on parameters.

5.2. *Non-specific quenching*

Our results show that the binding of TNP–ADP to the Na^+/K^+-ATPase is comprised of two parts; saturable binding to a single specific site, and non-specific binding which is not saturable out to 50 μM TNP–ADP. In addition, the amount of quenching due to non-specific binding of the TNP-nucleotide becomes substantial as the concentration of TNP-nucleotide is increased. Fig. 7 shows the fraction of the quenching due to non-specific binding of TNP–ADP as a function of the active fraction of enzyme for various concentrations of TNP–ADP. The curves are calculated using Eq. (6) with non-specific binding parameters of $q = 0.033$ and $a = 0.6$. Also shown are the values measured from the titration data including Figs. 3 and 5. Note that as the TNP–ADP concentration is increased beyond the amount needed to saturate the specific site, the contribution of non-specific binding to the quenching becomes increasingly important. Substantial error is introduced if non-specific binding is ignored in the analysis of titrations which go beyond 1 μM TNP–ADP. Also note in Fig. 7 that quenching due to non-specific binding is more important for the less active enzyme. This is because the inactive enzyme binds TNP–ADP non-specifically but not specifically in this model. These findings are consistent with those of Moczydlowski and Fortes [5] who saw non-specific binding of TNP–ATP to Na^+/K^+-ATPase which was non-saturable to 50 μM TNP–ATP. They are also similar to Tran and Farley [20] who found that 3′-O-(4-benzoyl)benzoyl-ATP binds to two classes of sites on Na^+/K^+-ATPase: a single high affinity site, and a low affinity site of undetermined high capacity.

The results from the ADP chase shown in Fig. 4 also support the existence of specific and non-specific binding. When ADP is added to a 10 μM TNP–ADP solution of enzyme, the ADP is able to displace TNP–ADP from the specific sites, but not from the non-specific sites. Thus the fluorescence recovers from 63% to about 80% of the initial unquenched value. Fig. 4 shows the data and the predicted recovery using the best fit parameters from Table 1 for the single site plus non-saturable non-specific binding model.

Table 1 shows that the equilibrium constant for the specific binding of TNP–ADP to the enzyme is about 0.1 μM, a value where the quenching due to non-specific binding accounts for 5–10% of the total quenching. Therefore, the nucleotide binding site becomes saturated at TNP–ADP concentrations where the fraction of quenching due to non-specific binding is still small. However, there is no reason why the equilibrium constant for a TNP-nucleotide must be low enough for the effects of non-specific binding to be unimportant. For example, preliminary results show that under the same conditions used for the TNP–ADP titrations, the equilibrium constant for TNP–ATP is about 2 μM. A titration out to 10 times this value is in the range where, according to Fig. 7, TNP–ADP non-specific binding accounts for 30–40% of the quenching. Another situation where non-specific binding may be important is if the enzyme is investigated in a state of its cycle in which the specific nucleotide binding site has low affinity. Then most of the quenching may be due to non-specifically bound TNP-nucleotide.

An equation for the fluorescence quenching due to non-specific binding of TNP–ADP to enzyme can be obtained from Eq. (6) by setting $k_1 = 0$. The resulting equation is

$$F = \frac{1}{1 + qT^a} \tag{10}$$

where from Table 1, q is around 0.033 and a is around 0.6. Given a measured level of quenched fluorescence, this equation can easily be used to determine how much of the quenching is due to non-specifically bound TNP-nucleotide. This equation, using best fit values, is plotted in Fig. 3d and Fig. 5c along with the data and best fits to the single site plus non-saturable non-specific binding model. Note that in both cases this non-specific quenching curve is close to the curve for the case where the specific binding sites are blocked by the presence of a high concentration of ADP.

The best fit value for parameter a of about 0.6 suggests that there is a distribution of affinities for non-specific binding. (A value of 1 corresponds to non-specific binding being proportional to the bulk concentration in which case all non-specific binding has the same affinity.) However, this model does not separate the cause of the non-specific quenching into the contribution made by the efficiency of the quenching versus the number of non-specific quenchers.

6. Conclusion

We find that a model with a single nucleotide binding site is insufficient for describing the interaction of TNP-nucleotide with Na^+/K^+-ATPase. Additional binding of TNP-nucleotide to the enzyme is needed to fully account for the fluorescence quenching. This additional binding is best characterized as non-saturable and non-specific, where our definition is that non-specific binding of TNP-nucleotide is not blocked by or affected by unlabelled nucleotide. This result is similar to some of the evidence for a distinct second nucleotide binding site, in particular that TNP–ADP binds to fluorescein isothiocyanate labelled enzyme [11,12]. It may be that this binding at a second site is the additional binding reported here, the only difference being that our definition of specificity is based on whether unlabelled nucleotide competes, versus a definition based on inhibition of phosphatase activity. For our purposes, the important point is to be able to separate the effects of this additional binding from the effects of binding at the high affinity site, in particular when analyzing transient kinetic stopped flow fluorescence quenching data ([3], submitted).

Acknowledgements

We thank Anu Palit, Bryan Yacono, and Jennifer M. Fox for the purification of the enzyme, Joe Robinson for critically reading the manuscript, and Terry Hawk of Duke Medical Center for support. Supported by a grant from the National Institutes of Health (GM-47550).

Appendix A

Here, we give the details of the derivations of the models for the fluorescence of IAF-labelled enzyme being quenched by TNP-nucleotide in the presence of unlabelled nucleotide. The procedure is the same for all of the models. In each case, the enzyme can be in a variety of states defined by the types of nucleotide bound to the enzyme. Each of these states has a particular quenching. So the procedure is to determine how much enzyme is in each state, multiply by the appropriate quenching term, then add up the fluorescences from all the states.

Fluorescence in the presence of quenchers is determined by the relative rates of fluorophore deexcitation via energy transfer to quencher and fluorophore deexcitation in the absence of quencher, k_f. (k_f is the inverse of the fluorescence lifetime in the absence of quenchers.) For a fluorophore-labelled enzyme in the presence of quencher, the fluorescence normalized to the unquenched fluorescence is

$$F = \frac{k_f}{k_f + k_q} = \frac{1}{1 + k_s} \tag{11}$$

where k_q is the rate of deexcitation due to energy transfer to quencher, and k_s is this rate normalized by k_f. Each state of the enzyme has a value for k_s associated with it.

Some of the IAF-labelled enzyme may not be able to bind nucleotide at the specific binding site. This may be due to damage which occurs during the purification. Such enzyme is referred to as inactive enzyme and is included in the models.

A.1. Single site model

In the single site model, the fraction of active enzyme which has a TNP-nucleotide at the specific binding site is

$$\frac{\dfrac{T}{Kt}}{1 + \dfrac{T}{Kt} + \dfrac{A}{Ka}} \tag{12}$$

Here, T is the concentration of TNP-nucleotide, A is the concentration of unlabelled nucleotide, and Kt and Ka are their respective equilibrium binding constants. The normalized energy transfer deexcitation rate for this state of the enzyme is k_f. The fraction of the active enzyme with either unlabelled nucleotide bound or no nucleotide bound has numerator

$$1 + \frac{A}{Ka} \tag{13}$$

and the same denominator as Eq. (12). This enzyme, along with the inactive enzyme (which cannot bind any TNP-nucleotide in this model) all have normalized energy transfer deexcitation rates of zero. Multiplying each fraction by the normalized fluorescence of Eq. (11) using the appropriate value for k_s, and adding them together results in the normalized fluorescence for the single site model, Eq. (3). The first term is the fluorescence from inactive enzyme and the second term is fluorescence from active enzyme. The fraction of active enzyme is xa.

A.2. Two-site model

For the two-site model, the enzyme has two specific nucleotide binding sites, each with its own affinity constants for the unlabelled nucleotide, Ka_1 and Ka_2, and the TNP-nucleotide, Kt_1 and Kt_2, and its own

quenching parameters, k_1 and k_2. This model has no non-specific binding. The fraction of active enzyme which has no TNP bound and hence has no quenching ($k_s = 0$) is

$$\frac{1 + \frac{A}{Ka_1} + \frac{A}{Ka_2} + \frac{A^2}{Ka_1 Ka_2}}{1 + \frac{A}{Ka_1} + \frac{A}{Ka_2} + \frac{A^2}{Ka_1 Ka_2} + \frac{T}{Kt_1} + \frac{T}{Kt_1}\frac{A}{Ka_2} + \frac{T}{Kt_2} + \frac{A}{Ka_1}\frac{T}{Kt_2} + \frac{T^2}{Kt_1 Kt_2}} \tag{14}$$

Eq. (14) is the sum of enzyme fractions where both sites are empty, or one or both sites have unlabelled nucleotide bound. The rest of the fractions for this model all have the same denominator as Eq. (14). The fraction of active enzyme with a TNP bound only at site 1 and quenching with $k_s = k_1$ has numerator

$$\frac{T}{Kt_1} + \frac{T}{Kt_1}\frac{A}{Ka_2} \tag{15}$$

The fraction with a TNP bound only at site 2 and quenching $k_s = k_2$ has numerator

$$\frac{T}{Kt_2} + \frac{A}{Ka_1}\frac{T}{Kt_2} \tag{16}$$

The fraction with quenching due to TNP at both sites and $k_s = k_1 + k_2$ has numerator

$$\frac{T^2}{Kt_1 Kt_2} \tag{17}$$

Adding together the fluorescences from all the states of the enzyme and including the inactive enzyme gives the normalized fluorescence for the two-site model, Eq. (4).

A.3. Single site plus saturable non-specific binding model

In this model, in addition to the single specific site which unlabelled and TNP-labelled nucleotide compete for on active enzyme, one TNP-nucleotide may bind non-specifically to both active and inactive enzyme. The single specific site is specified by the parameters Ka_1, Kt_1, and k_1. The saturable non-specific binding of TNP-nucleotide is specified by an equilibrium binding constant Kt_2 and a normalized energy transfer deexcitation rate k_2. The fraction of active enzyme with no TNP bound and $k_s = 0$ is

$$\frac{1 + \frac{A}{Ka_1}}{1 + \frac{A}{Ka_1} + \frac{T}{Kt_1} + \frac{T}{Kt_2} + \frac{A}{Ka_1}\frac{T}{Kt_2} + \frac{T^2}{Kt_1 Kt_2}} \tag{18}$$

The fraction of active enzyme with TNP bound at the specific site only and $k_s = k_1$ has the same denominator as Eq. (18) and numerator

$$\frac{T}{Kt_1} \tag{19}$$

The fraction of active enzyme with TNP bound non-specifically only and $k_\times = k_2$ has the same denominator as Eq. (18) and numerator

$$\frac{T}{Kt_2} + \frac{A}{Ka_1}\frac{T}{Kt_2} \tag{20}$$

The fraction of active enzyme with TNP bound both specifically and non-specifically and $k_\times = k_1 + k_2$ has the same denominator as Eq. (18) and numerator

$$\frac{T^2}{Kt_1 Kt_2} \tag{21}$$

The fraction of inactive enzyme with no TNP non-specifically bound and $k_\times = 0$ is

$$\frac{1}{1 + \dfrac{T}{Kt_2}} \tag{22}$$

The fraction of inactive enzyme with TNP non-specifically bound and $k_\times = k_2$ has the same denominator as Eq. (22) and numerator

$$\frac{T}{Kt_2} \tag{23}$$

Adding the fluorescences from all the states of the enzyme results in Eq. (5).

A.4. Single site plus non-saturable non-specific binding

In this model, in addition to the single specific site which unlabelled and TNP-labelled nucleotide compete for on the active enzyme, there is also non-saturable non-specific binding of TNP-nucleotide to both active and inactive enzyme. Energy transfer from the IAF label to non-specifically bound TNP–ADP provides an additional process for fluorophore deexcitation. We use a simple two parameter characterization in which the normalized rate of deexcitations due to energy transfer to non-specifically bound TNP-nucleotide is qT^a where T is the concentration of TNP–ADP in solution. This form is justified as follows.

The net rate for deexcitation due to energy transfer to non-specifically bound TNP-nucleotide is obtained by adding the deexcitation rates due to energy transfer to each individual non-specifically bound TNP-ADP. For simplicity, we assume that each of these individual rates is the same, so that the net rate is then proportional to the amount of non-specifically bound TNP–ADP. Typically, if non-specific binding is included at all in a model, it is modelled by making the amount of non-specifically bound ligand be linearly proportional to the concentration free in solution [14,15]. However, we choose to make this amount be proportional to the concentration in solution raised to the power a. For $a < 1$, this provides us with a simple parameterization which has the desirable features that a plot of the amount of non-specifically bound ligand versus the free concentration has a negative curvature and no limit, as would be expected if the non-specific binding is heterogeneous and non-saturable. If the non-specific binding sites are all identical and hence, have a single affinity then $a = 1$ and our model becomes the simpler linearly proportional model. The two parameters in our model are the proportionality constant q and the power a to which the concentration of TNP–ADP in solution is raised. q is related to the quenching efficiency and the density of non-specific sites, and a is related to the distribution of affinities of the non-specific sites. Although our treatment of non-specific binding is still

oversimplified, it does contain the desirable features of non-saturability and heterogeneity of non-specific binding.

The fraction of active enzyme which has no TNP-nucleotide specifically bound is

$$\frac{1+\frac{A}{Ka}}{1+\frac{A}{Ka}+\frac{T}{Kt}} \tag{24}$$

This enzyme has quenching due only to non-specific binding so $k_s = qT^a$. The fraction of active enzyme with TNP-nucleotide specifically bound has the same denominator as Eq. (24) and numerator

$$\frac{T}{Kt} \tag{25}$$

This enzyme has quenching due to both specifically bound and non-specifically bound TNP-nucleotide so $k_s = k_1 + qT^a$. The inactive enzyme has quenching due to non-specific binding with $k_s = qT^a$. Adding the fluorescences from all the states of the enzyme results in Eq. (6), where xa is the fraction of enzyme which is capable of specifically binding TNP-nucleotide, Kt and Ka are the equilibrium dissociation constants for TNP labelled and unlabelled nucleotide, q and a are the non-specific quenching parameters described above, and k_1 is the normalized specific binding energy transfer rate.

References

[1] J.C. Skou, Methods Enzymol. 156 (1988) 1–25.
[2] I.M. Glynn, J. Physiol. 462 (1993) 1–30.
[3] P.R. Pratap, A. Palit, E.H. Hellen, J.D. Robinson, Biophys. J. 70 (1996) A325.
[4] P.A.G. Fortes, R. Aguilar, Prog. Clin. Biol. Res. 268A (1988) 197–204.
[5] E.G. Moczydlowski, P.A.G. Fortes, J. Biol. Chem. 256 (1981) 2346–2356.
[6] E.G. Moczydlowski, P.A.G. Fortes, J. Biol. Chem. 256 (1981) 2357–2366.
[7] E. Amler, A. Abbott, W.J. Ball Jr, Biophys. J. 61 (1992) 553–568.
[8] M. Moutin, M. Cuillel, C. Rapin, R. Miras, M. Anger, A. Lompre, Y. Dupont, J. Biol. Chem. 269 (1994) 11147–11154.
[9] M.B. Murataliev, P.D. Boyer, J. Biol. Chem. 269 (1994) 15431–15439.
[10] E. Capieaux, C. Rapin, D. Thines, Y. Dupont, A. Goffeau, J. Biol. Chem. 268 (1993) 21895–21900.
[11] D.G. Ward, J.D. Cavieres, J. Biol. Chem. 271 (1996) 12317–12321.
[12] G. Scheiner-Bobis, J. Antonipillai, R.A. Farley, Biochemistry 32 (1993) 9592–9599.
[13] A. Askari, J. Bioenerg. Biomembr. 19 (1987) 359–374.
[14] D.A. Lauffenburger, J.J. Linderman, Receptors, Oxford Univ. Press, New York, 1993.
[15] P.A.G. Fortes, Anal. Biochem. 158 (1986) 454–462.
[16] P.L. Jørgensen, Biochim. Biophys. Acta 356 (1974) 36–52.
[17] J.G. Kapakos, M. Steinberg, Biochim. Biophys. Acta 693 (1982) 493–496.
[18] M. Steinberg, S.J.D. Karlish, J. Biol. Chem. 264 (1989) 2726–2734.
[19] U. Banik, S. Roy, Biochem. J. 266 (1990) 611–614.
[20] C.M. Tran, R.A. Farley, Biochem. Biophys. Acta 860 (1986) 9–14.